Structural Engineering and Mechanics, Vol. 34, No. 6 (2010) 667-683
DOI: http://dx.doi.org/10.12989/sem.2010.34.6.667

Analytical solution of two-layer beam including interlayer slip and uplift

Aleš Kroflič, Igor Planinc, Miran Saje* and Bojan Čas

University of Ljubljana, Faculty of Civil and Geodetic Engineering, Jamova 2, SI-1115 Ljubljana, Slovenia

(Received July 14, 2008, Accepted December 7, 2009)

Abstract. A mathematical model and its analytic solution for the analysis of stress-strain state of a linear elastic two-layer beam is presented. The model considers both slip and uplift at the interface. The solution is employed in assessing the effects of transverse and shear contact stiffnesses and the thickness of the interface layer on behaviour of nailed, two-layer timber beams. The analysis shows that the transverse contact stiffness and the thickness of the interface layer have only a minor influence on the stress-strain state in the beam and can safely be neglected in a serviceability limit state design.

Keywords: composite beam; slip; uplift; analytical solution; elasticity; parametric study.

1. Introduction

Layered beams belong to a group of innovative structural elements, usually classified as composite structures, whose usage increases in all branches including civil engineering. There is a number of good reasons for such an increase (Čas *et al.* 2004a, Oehlers *et al.* 1997, Pendhari *et al.* 2006, Salari *et al.* 1998). The application of composite beams is widespread in designing both new structures and in the rehabilitation of existent constructions.

The basic theories of composite beams were developed in the middle of the last century after a number of experimental observations had confirmed that the flexible contact between the layers played an important role in behaviour. An extensive overview of the early experimental work was presented by Viest (1960). The first mathematical theories of flexibly connected layers of composite beams were developed independently in Sweden (Granholm 1949), Russia (Pleshkov 1952), Switzerland (Stüssi 1947) and in the United States of America (Newmark 1951). Most of subsequent theories consider linear elastic behaviour and small displacements (Suzuki and Chang 1979, Girhammar and Gopu 1993, Nie and Cai 2003, Ranzi *et al.* 2003, Sun and Bursi 2005, Schnabl *et al.* 2006, 2007a, Xu and Wu 2007). A number of theories also consider some non-linearity, as, e.g., Rassam and Goodman (1970), Thompson *et al.* (1975), Hirst and Yeo (1980), Betti and Gjelsvik (1996), Wang (1998), Salari *et al.* (1998, 2001), Fabbrocino *et al.* (1999, 2000), Gattesco (1999), Van der Linden (1999), Manfredi *et al.* (1999), Milner and Tan (2001), Nguyen *et*

*Corresponding author, Professor, E-mail: msaje@fgg.uni-lj.si

al. (2001), Rahimi and Hutchinson (2001), Seracino *et al.* (2001), Rasheed and Pervaiz (2002), Ayoub (2005), who considered material non-linearities, and Wheat and Calixo (1994), Čas *et al.* (2004b), Girhammar and Pan (2007), Ranzi and Bradford (2007), who took into account both material and geometric non-linearities, yet in a rather simplified manner. Čas *et al.* (2004a) seems to be the first to introduce a fully consistent materially and geometrically non-linear model of composite engineering beams.

The majority of the analysis procedures take into consideration solely an interlayer slip between the layers neglecting uplift. The mathematical models that consider both slip and uplift in the contact were proposed only by Adekola (1968), Robinson and Naraine (1988) and Gara *et al.* (2006). Their mathematical models consider geometrically and materially linear behaviour (Adekola 1968, Robinson and Naraine 1988), or a bilinear constitutive law of materials (Gara *et al.* 2006).

This paper discusses the effect of slip and uplift at the contact interface on mechanical behaviour of two-layer elastic beams considering the geometrically linear planar beam theory. In particular, we investigate a combined effect of slip and uplift on the stress and strain state. The linear shear force-slip and transverse force-uplift relationships are considered for shear connectors. The contact of layers where slip and uplift actually occur, is modelled with an additional fictitious layer of small thickness.

Finally, an engineering analysis of behaviour of a nailed, two-layer, timber, simply supported beam is presented, in which the given distribution of forces in connectors as a function of shear and transverse stiffnesses as well as the thickness of the connecting layer is believed to be of a particular interest to designers.

2. Mathematical model of a two-layer composite beam

For the sake of simplicity of the derivation, only a two-layer beam is considered (Fig. 1). The equations of a multi-layer beam can be derived similarly.

We assume that each layer suffers small deformations, so that the geometrically linear beam model is sufficient (Fig. 2). The material is assumed to be linear elastic.

During deformation, the layers slip over each other and may separate. If layers are very stiff compared to connectors, or if they are not connected, both slip and uplift occur at the contact. If one layer is much softer than the other or if both layers are nearly as stiff as the connectors, slip and uplift are small and can thus be attributed to a thin connecting layer.

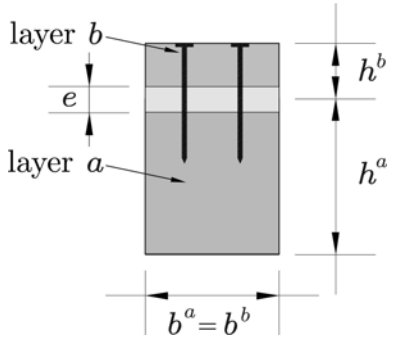

Fig. 1 Cross-section of a typical two-layer beam

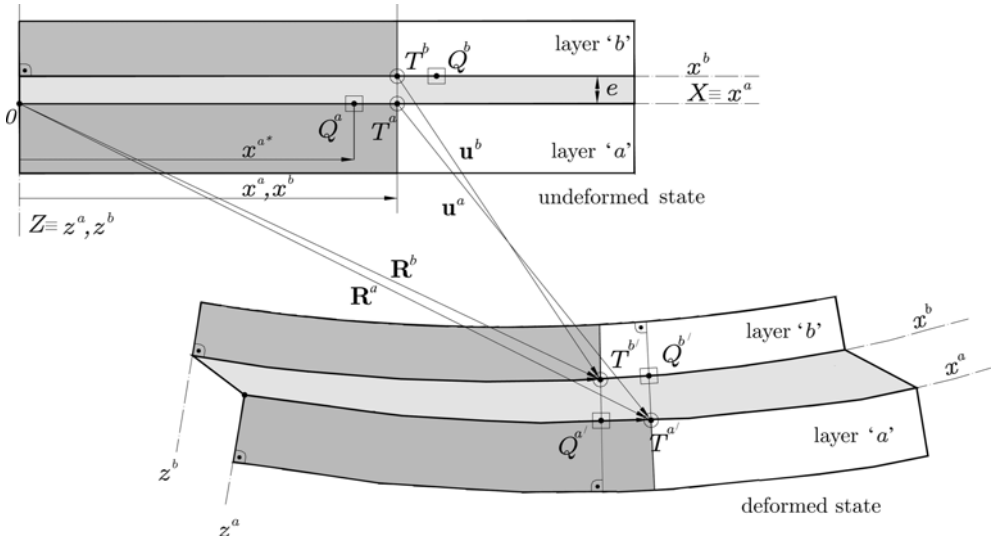

Fig. 2 Undeformed and deformed configurations of a composite beam

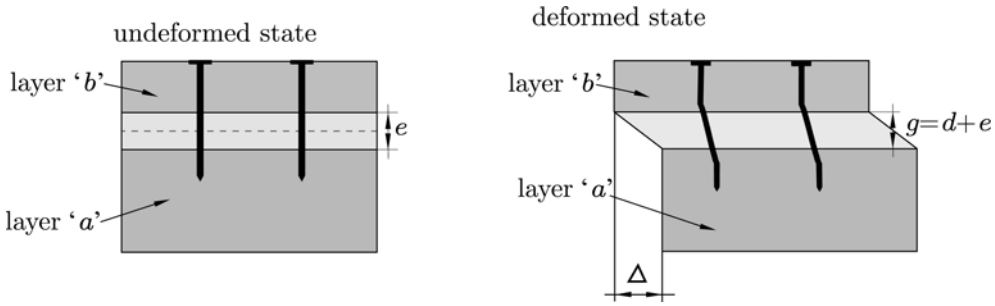

Fig. 3 Geometrical meaning of slip (Δ) and uplift (*d*)

For this reason, slip and uplift are in the present paper defined in a generalized way as an 'average slip' and an 'average uplift' over a thin connecting layer of a softer material rather than slip and the uplift over an actual contact surface (Fig. 3). Hence, the interaction between layers '*a*' and '*b*' is realized through the connecting layer of thickness *e*, thus being more a computational than a geometric property, yet depending on actual characteristics of layers and connectors. The thickness *e* and other material parameters of the connecting layer must be obtained in a specially designed experiment using the method of the inverse analysis (see e.g., Koc and Štok 2004). Once identified in experiment, the generalized slip (uplift) is used in a force-slip (uplift) relationship. The shear force-slip and the transverse force-uplift relationships are here assumed to be linear, which is a reasonable assumption when displacements are small. The introduction of such a generalized type of slip and uplift seems to be physically sound and adds an additional material parameter, *e*, to the mathematical model.

Bernoulli's hypothesis of planar cross-sections is assumed for each layer. Shear strains are neglected, which is a reasonable assumption for long beams (Schnabl *et al*. 2007b). Each layer is assumed to behave like a planar beam, but is constrained to be connected to the other layer by the connecting layer. The static equilibrium of the composite beam is thus governed by the system of

kinematic, equilibrium and constitutive equations for each layer supplemented by their natural and essential boundary conditions, and the conditions of the connection. It is assumed that the tangential surface traction at the interface is proportional to slip, while the transverse surface traction is proportional to uplift. In what follows we first present an overview of the governing equations of the model of the two-layer beam. Further details of the derivation are given in, e.g., Adekola (1968), Gara *et al.* (2006) and Robinson and Naraine (1988).

Kinematic equations

$$\begin{aligned} u^{a\prime} - \varepsilon^a &= 0 & u^{b\prime} - \varepsilon^b &= 0 \\ w^{a\prime} + \varphi^a &= 0 & w^{b\prime} + \varphi^b &= 0 \\ \varphi^{a\prime} - \kappa^a &= 0 & \varphi^{b\prime} - \kappa^b &= 0 \end{aligned} \tag{1}$$

Equilibrium equations

$$\begin{aligned} N^{a\prime} + \mathscr{P}_x^a &= 0 & N^{b\prime} + \mathscr{P}_x^b &= 0 \\ Q^{a\prime} + \mathscr{P}_z^a &= 0 & Q^{b\prime} + \mathscr{P}_z^b &= 0 \\ M^{a\prime} - Q^a + \mathscr{M}_y^a &= 0 & M^{b\prime} - Q^b + \mathscr{M}_y^b &= 0 \end{aligned} \tag{2}$$

Constitutive equations

$$\begin{aligned} N^a &= C_{11}^a \varepsilon^a + C_{12}^a \kappa^a & N^b &= C_{11}^b \varepsilon^b + C_{12}^b \kappa^b \\ M^a &= C_{21}^a \varepsilon^a + C_{22}^a \kappa^a & M^b &= C_{21}^b \varepsilon^b + C_{22}^b \kappa^b \end{aligned} \tag{3}$$

Constraining conditions

$$\Delta = u^a - u^b - e\,\varphi^a \tag{4}$$

$$x^b + u^b = x^{a*} + u^a - e\,\varphi^a \tag{5}$$

$$d = w^a - w^b - e \tag{6}$$

$$p_t = K\Delta \tag{7}$$

$$p_n = Cd \tag{8}$$

In the above equations, indices 'a' and 'b' mark that the function belong to layer 'a' or 'b' (Fig. 5). Kinematic Eq. (1) of each layer link basic kinematic quantities $(u^a, u^b, w^a, w^b, \varphi^a, \varphi^b)$ and deformation quantities $(\varepsilon^a, \varepsilon^b, \kappa^a, \kappa^b)$. Equilibrium Eqs. (2) of each layer represent relationships between the internal static quantities $(N^a, N^b, Q^a, Q^b, M^a, M^b)$ and loading over the layers $(\mathscr{P}_x^a, \mathscr{P}_x^b, \mathscr{P}_z^a, \mathscr{P}_z^b, \mathscr{M}_y^a, \mathscr{M}_y^b)$. Loading in Eq. (2) consists of the external loading on the composite beam (p_x^a, p_z^a) and contact forces (p_t, p_n) at the interface

$$\begin{aligned} \mathscr{P}_x^a &= p_x^a - p_t \\ \mathscr{P}_x^b &= p_x^b + p_t \\ \mathscr{P}_z^a &= p_z^a - p_n \\ \mathscr{P}_z^b &= p_z^b + p_n \end{aligned} \tag{9}$$

The meaning of the axial contact traction p_t and the vertical contact traction p_n in Eq. (9) is depicted in Fig. 4. $\mathscr{M}_y^a$ and $\mathscr{M}_y^b$ are moment tractions. The constants C_{jk}, $j,k = 1,2$, in Eq. (3) denote the coefficients of the cross-sectional tangent matrix: $C_{11}^i = \int_{A^i} E^i dA^i$ is the axial tangent cross-sectional stiffness of layer i, $C_{12}^i = C_{21}^i = \int_{A^i} z E^i dA^i$ describe the coupling of axial and bending strains of the beam, and $C_{22}^i = \int_{A^i} z^2 E^i dA^i$ is the bending cross-sectional stiffness of layer i, where $i = a, b$. Constraining conditions (4)-(8) consist of two separate sets of equations. The first set comprises Eqs. (4)-(6) representing kinematic conditions of constraint.

The meaning of the quantities introduced in Eqs. (4)-(6) can be clearly recognized from Fig. 5.

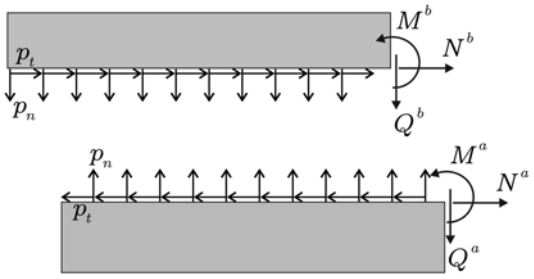

Fig. 4 Meaning of unknowns of Eq. (2)

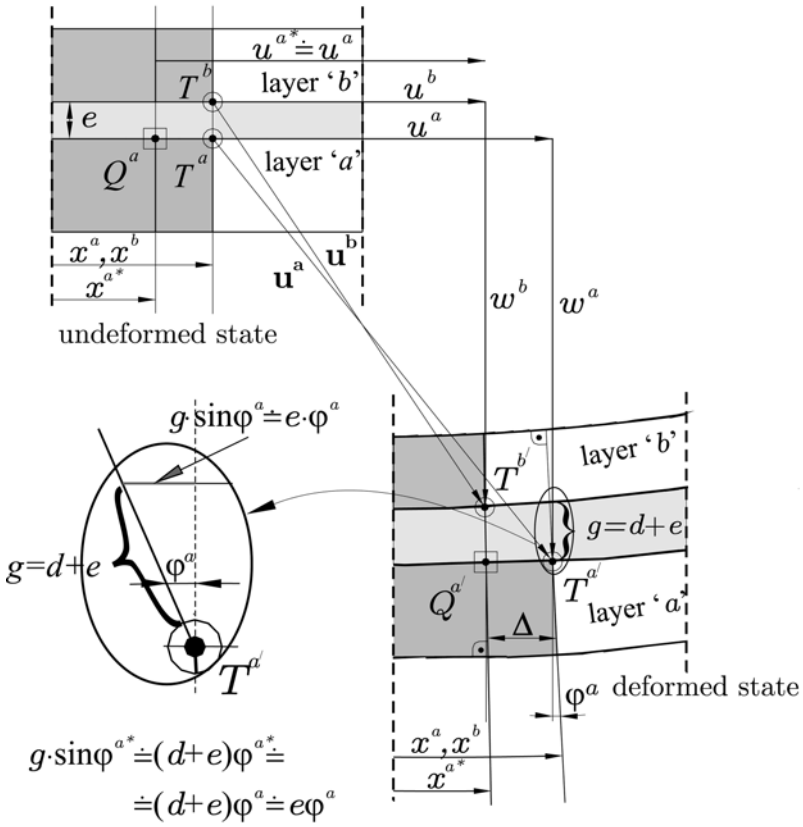

Fig. 5 Geometrical meaning of kinematical unknowns of Eqs. (4)-(6)

There are two new kinematic quantities, slip, Δ, and uplift, d, introduced and related to shear surface traction p_t and transverse surface traction p_n by Eqs. (7) and (8). There the coefficients K and C represent the linearized contact stiffnesses in the axial and transverse direction, respectively.

The system of Eqs. (1)-(8) consists of 21 equations which must be solved for 21 unknowns u^a, w^a φ^a, $u^b, w^b, \varphi^b, N^a, Q^a, M^a, N^b, Q^b, M^b, \varepsilon^a, \kappa^a, \varepsilon^b, \kappa^b, \Delta, d, x^{a*}, p_t$ and p_n. A systematic elimination of unknowns from Eqs. (1)-(8) gives a single ordinary differential equation of seventh order with constant coefficients for slip

$$\Delta^{(VII)} - k_1\Delta^{(V)} - k_5\Delta^{(''')} + (k_5k_1 - k_2k_4)\Delta' + k_5k_3 - k_2k_6 = 0 \tag{10}$$

Its characteristic equation is (Deo and Ragmavendra 1994)

$$y^7 - k_1y^5 - k_5y^3 + (k_5k_1 - k_2k_4)y + k_5k_3 - k_2k_6 = 0 \tag{11}$$

An extensive parametric analysis has revealed that the above polynomial has 3 real and 2 conjugate complex zeros for the range of material parameters in structural engineering. The real zeros are denoted r_1, r_2, r_3, while the complex ones are denoted $c_1 = \alpha_1 + \alpha_2 i$, $\bar{c}_1 = \alpha_1 - \alpha_2 i$, $c_2 = \beta_1 + \beta_2 i$, $\bar{c}_2 = \beta_1 - \beta_2 i$, where $i = \sqrt{-1}$.

Thus, the general solution of the differential Eq. (10) is (Deo and Ragmavenda 1994)

$$\Delta(x) = C_1e^{r_1x} + C_2e^{r_2x} + C_3e^{r_3x} + e^{\alpha_1x}(C_4\cos\alpha_2x + C_5\sin\alpha_2x) + e^{\beta_1x}(C_6\cos\beta_2x + C_7\sin\beta_2x) \tag{12}$$

The integration constants, C_1, C_2, C_3, C_4, C_5, C_6 and C_7, are obtained from the boundary conditions at $x = 0$ for slip, uplift, the first two derivatives of slip and the first three derivatives of uplift (Fig. 5):

$$\Delta(0) = u^a(0) - u^b(0) - e\varphi^a(0) \tag{13}$$

$$\Delta'(x) = \varepsilon^a - \varepsilon^b - e\kappa^a \rightarrow \Delta'(0) =$$
$$D_{11}^aN^a(0) + D_{12}^aM^a(0) - D_{11}^bN^b(0) - D_{12}^bM^b(0) - eD_{21}^aN^a(0) - eD_{22}^aM^a(0) \tag{14}$$

$$\Delta''(x) = -(eD_{21}^a - D_{11}^a - D_{11}^b)K[u^a(0) - u^b(0) - e\varphi^a(0)] + (D_{12}^a - eD_{22}^a)Q^a(0) - D_{12}^aQ^b(0) \tag{15}$$

$$d(0) = w^a(0) - w^b(0) - e \tag{16}$$

$$d'(0) = \varphi^b(0) - \varphi^a(0) \tag{17}$$

$$d''(x) = \kappa^b - \kappa^a = D_{21}^bN^b(x) + D_{22}^bM^b(x) - D_{21}^aN^a(x) - D_{22}^aM^a(x) \rightarrow$$
$$\rightarrow d''(0) = D_{21}^aN^b(0) + D_{22}^bM^b(0) - D_{21}^aN^a(0) - D_{22}^aM^a(0) \tag{18}$$

$$d'''(0) = -(D_{21}^a + D_{21}^b)K\Delta(0) + D_{22}^bQ^b(0) - D_{22}^aQ^a(0) \tag{19}$$

Coefficients D_{ij} introduced above are the components of the cross-sectional compliance matrix

$$\begin{bmatrix} \begin{bmatrix} D_{11}^a & D_{12}^a \\ D_{21}^a & D_{22}^a \end{bmatrix} & \begin{matrix} 0 & 0 \\ 0 & 0 \end{matrix} \\ \begin{matrix} 0 & 0 \\ 0 & 0 \end{matrix} & \begin{bmatrix} D_{11}^b & D_{12}^b \\ D_{21}^b & D_{22}^b \end{bmatrix} \end{bmatrix} = \begin{bmatrix} \begin{bmatrix} C_{11}^a & C_{12}^a \\ C_{21}^a & C_{22}^a \end{bmatrix}^{-1} & \begin{matrix} 0 & 0 \\ 0 & 0 \end{matrix} \\ \begin{matrix} 0 & 0 \\ 0 & 0 \end{matrix} & \begin{bmatrix} C_{11}^b & C_{12}^b \\ C_{21}^b & C_{22}^b \end{bmatrix}^{-1} \end{bmatrix} \tag{20}$$

Zero external moment traction over the beam and the relations

$$\begin{aligned} \varepsilon^a &= D_{11}^a N^a + D_{12}^a M^a \\ \kappa^a &= D_{21}^a N^a + D_{22}^a M^a \\ \varepsilon^b &= D_{11}^b N^b + D_{12}^b M^b \\ \kappa^b &= D_{21}^b N^b + D_{22}^b M^b \end{aligned} \tag{21}$$

obtained by inverting Eq. (3) were employed in deriving Eqs. (14), (15), (18) and (19). When needed the derivatives $N^{a\prime}$, $N^{b\prime}$, $Q^{a\prime}$, $Q^{b\prime}$, $M^{a\prime}$ and $M^{b\prime}$ are derived from the equilibrium Eq. (2)

$$\begin{aligned} N^{a\prime} &= -\mathscr{P}_x^a = -(p_x^a - p_t) = -(p_x^a - K\Delta) \\ N^{b\prime} &= -\mathscr{P}_x^b = -(p_x^b + p_t) = -(p_x^b + K\Delta) \\ Q^{a\prime} &= -\mathscr{P}_z^a = -(p_z^a - p_n) = -(p_z^a - Cd) \\ Q^{b\prime} &= -\mathscr{P}_z^b = -(p_z^b + p_n) = -(p_z^b + Cd) \\ M^{a\prime} &= Q^a \\ M^{b\prime} &= Q^b \end{aligned} \tag{22}$$

The boundary conditions associated with the above equations consist of static and kinematic conditions at the two ends of the beam as follows.

Static boundary conditions

- left end, $x = 0$

$$\begin{aligned} S_1^a + N^a(0) &= 0 \qquad & S_1^b + N^b(0) &= 0 \\ S_2^a + Q^a(0) &= 0 \qquad & S_2^b + Q^b(0) &= 0 \\ S_3^a + M^a(0) &= 0 \qquad & S_3^b + M^b(0) &= 0 \end{aligned} \tag{23}$$

- right end, $x = L$

$$\begin{aligned} S_4^a - N^a(L) &= 0 \qquad & S_4^b - N^b(L) &= 0 \\ S_5^a - Q^a(L) &= 0 \qquad & S_5^b - Q^b(L) &= 0 \\ S_6^a - M^a(L) &= 0 \qquad & S_6^b - M^b(L) &= 0 \end{aligned} \tag{24}$$

Kinematic boundary conditions

- left end, $x = 0$

$$\begin{aligned} u^a(0) &= U_1^a & u^b(0) &= U_1^b \\ w^a(0) &= U_2^a & w^b(0) &= U_2^b \\ \varphi^a(0) &= U_3^a & \varphi^b(0) &= U_3^b \end{aligned} \tag{25}$$

- right end, $x = L$

$$\begin{aligned} u^a(L) &= U_4^a & u^b(L) &= U_4^b \\ w^a(L) &= U_5^a & w^b(L) &= U_5^b \\ \varphi^a(L) &= U_6^a & \varphi^b(L) &= U_6^b \end{aligned} \tag{26}$$

In Eqs. (23)-(26) U_i^a and U_i^b $(i = 1, \ldots, 6)$ mark the given values of the boundary displacements, and S_i^a and S_i^b $(i = 1, \ldots, 6)$ the given values of the forces at the ends $x = 0$ and $x = L$ of layers a and b.

The exact solution was fully elaborated with Mathematica (Wolfram Research 2005). Once the analytical expression for slip as a function of x is obtained, the remaining unknowns are easily derived from Eqs. (1)-(8). The boundary values of unknowns and unknown integration constants are determined from the prescribed boundary conditions. Aftere these unknowns have been determined, the remaining unknown functions follow from Eqs. (1)-(8).

3. Two-layer timber composite beam: a parametric study

The objective of this section is to assess the effects of a contact transverse stiffness and the contact layer thickness on the stress-strain state of a nailed, two-layer timber beam. A simply supported timber beam of length $L = 280$ cm is studied. The beam has been recently experimentally and numerically analysed by Planinc *et al.* (2008). Deflections of the axis of the beam, slips at the contact and the following material characteristics of timber and the connection were measured in the experiment:

- compressive strength parallel to the grain,
- tensile strength parallel to the grain,
- shear stiffness and load bearing capacity of connectors,
- tensile drag characteristics of connectors.

The composite cross-section is presented in Fig. 6. In accordance with the Eurocode 5 (2004) classification, timber has been classified in strength class C24. The nails 4/100 were arranged in two parallel rows and uniformly distributed along the contact interface (Fig. 6).

Experiments showed that the shear resistance of one nail is $R_T = 0.77$ kN and its tensile drag resistance $R_N = 0.61$ kN. The short cantilevers at the supports (Fig. 6) have been neglected in mathematical modelling. Constant distances (9 cm) between the nails along the beam axis have been assumed.

The beam was subjected to self load and an external point load at the middle of the beam span. Measurements were performed for three stages of the point load (Eurocode 5 2004):

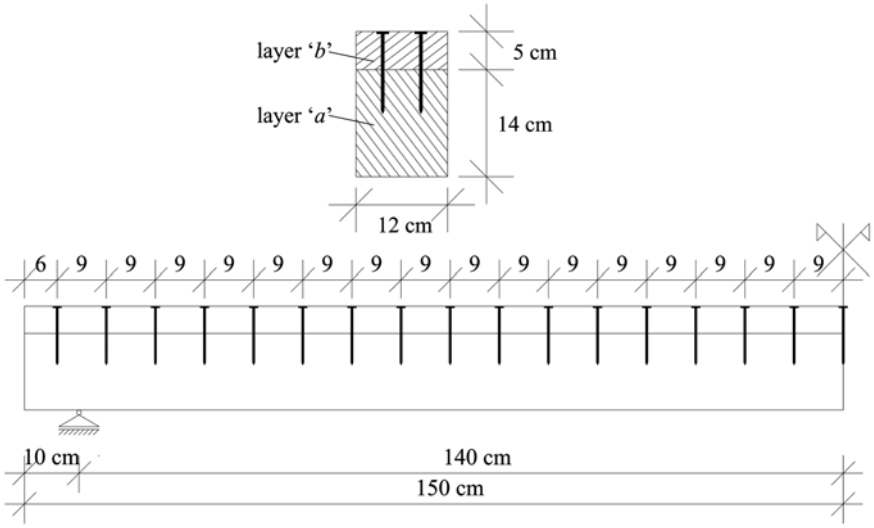

Fig. 6 Cross-section of composite timber beam and the arrangement of connectors

- characteristic load (P = 7.624 kN),
- design load (P = 11.055 kN) and
- ultimate load (P = 16.123 kN)

As our mathematical model considers linear elastic material model, its results could be realistic for the lowest load level only. The parameters of the constitutive law of timber were determined in a series of compressive and tensile tests on standard timber speciments. Only the linear part of the non-linear stress-strain response was used, yielding the value of modulus of elasticity to be E = 1500 kN/cm^2 and the maximum extensional elastic strain D = 0.52%.

The constitutive model of the nail shear resistance was also found non-linear and had to be linearized. Although the nails are discrete, the distributed connection with constant strength and stiffness properties has been employed in the model for comformity with our theoretical model of the beam. The related slip modulus was obtained by dividing the experimentally determined modulus of the nail by the distance between the nails and multiplied by the number of nails in the considered section yielding K = 2.448 kN/cm. Similarly, the constitutive law of the contact in the transverse direction was also found non-linear. After its linearization, and assuming equal behaviour in tension and compression, we obtain C = 8.93 kN/cm.

3.1 Effect of transverse stiffness of connecting layer

In the first step of our parametric analysis, we examine the influence of the transverse stiffness on the static and kinematic quantities in the nailed, two-layer timber beam. The range of the values of the transverse stiffness is presented in Table 1. The thickness of the connecting layer is taken to be e = 0 cm.

Table 1 Selected values of the transverse contact stiffness

Parameter	Selected values [kN/cm]				
C	∞	100 000	8.93 (experiment)	1	0.1

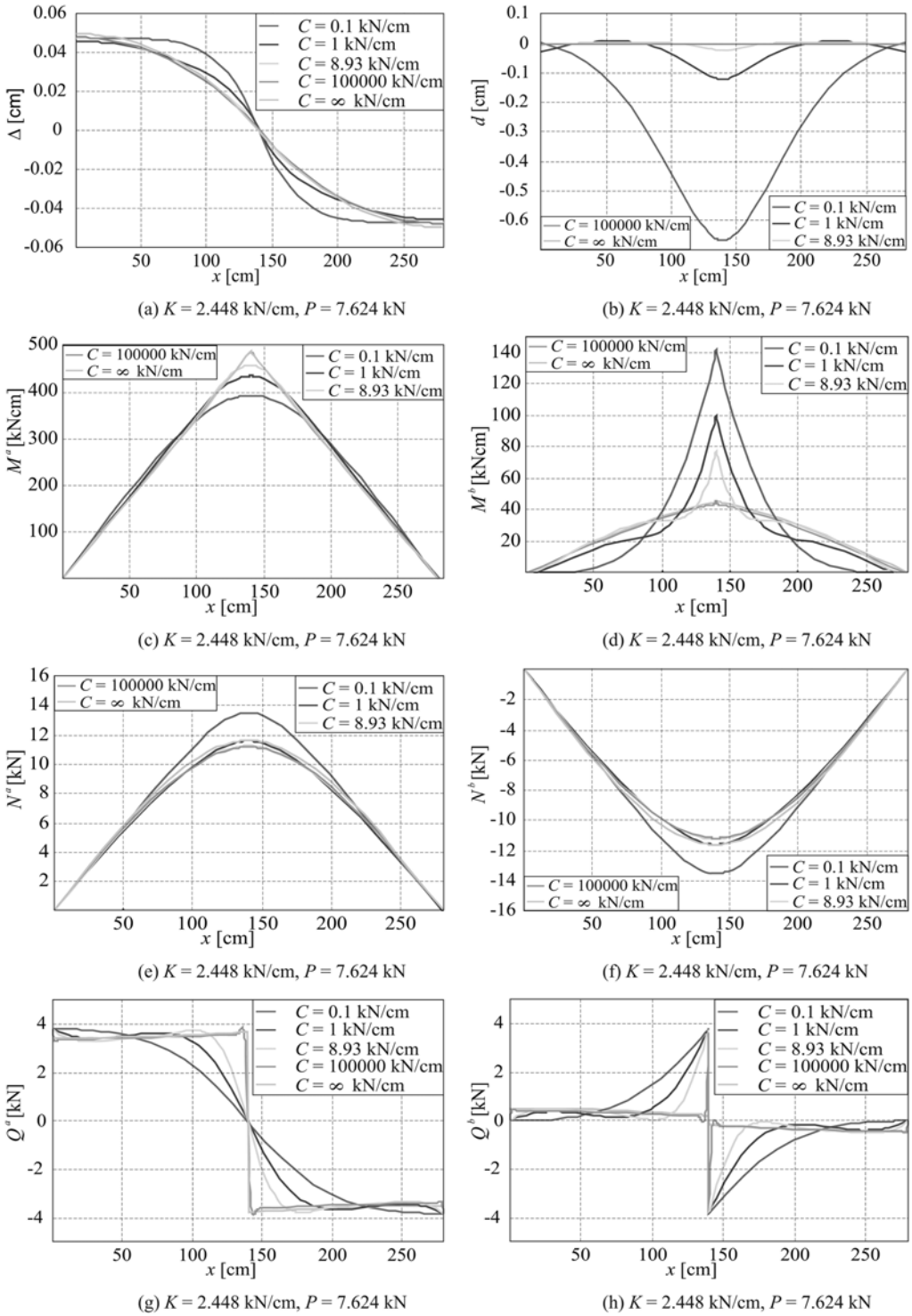

(a) $K = 2.448$ kN/cm, $P = 7.624$ kN

(b) $K = 2.448$ kN/cm, $P = 7.624$ kN

(c) $K = 2.448$ kN/cm, $P = 7.624$ kN

(d) $K = 2.448$ kN/cm, $P = 7.624$ kN

(e) $K = 2.448$ kN/cm, $P = 7.624$ kN

(f) $K = 2.448$ kN/cm, $P = 7.624$ kN

(g) $K = 2.448$ kN/cm, $P = 7.624$ kN

(h) $K = 2.448$ kN/cm, $P = 7.624$ kN

Fig. 7 Influence of the transverse contact stiffness on slip, uplift, axial and shear forces and bending moment in layers '*a*' and '*b*'

Fig. 7(a) presents the variation of slip along the contact surface for various values of the transverse contact stiffness. The influence of the transverse contact stiffness on slip is rather small. Its effect increases only in the central part of the beam when the value of the transverse contact stiffness is small. Fig. 7(b) depicts the variation of uplift along the contact. It can be clearly seen that the present model predicts that the upper layer penetrates into the lower one. As expected the largest penetration takes place just at the point of application of the load. The variation of bending moments in both the upper and the lower layer is displayed in Figs. 7(c) and 7(d). The maximum value of the bending moment in the lower layer decreases somewhat with the reduction of the transverse contact stiffness, while the shape of the graph tends to adapt from triangular to parabolic. Fig. 7(d) depicts changing of the bending moment in the upper layer. Here, both the quantitative and qualitative differences are notable. Observe an intensive, peak-like increase in the bending moment at the point of application of the load for a small transverse contact stiffness. Figs. 7(e) and 7(f) present the graphs of the variation of the axial load. Here the efect of transverse contact stiffness is small. In contrast, the effect of the transverse contact stiffness on the magnitude and variation of shear forces in longitudinal direction is important, as shown in Figs. 7(g) and 7(h). In particular, the value of the shear force in the central section of the upper layer differs a lot for the range of low transverse contact stiffnesses.

3.2 Effect of thickness of connecting layer

The analysis was carried out for three thicknesses: 0 cm, 0.5 cm, 1 cm. The subplots of Fig. 8 show the slip variation over the length of the contact as a function of the layer thickness and the

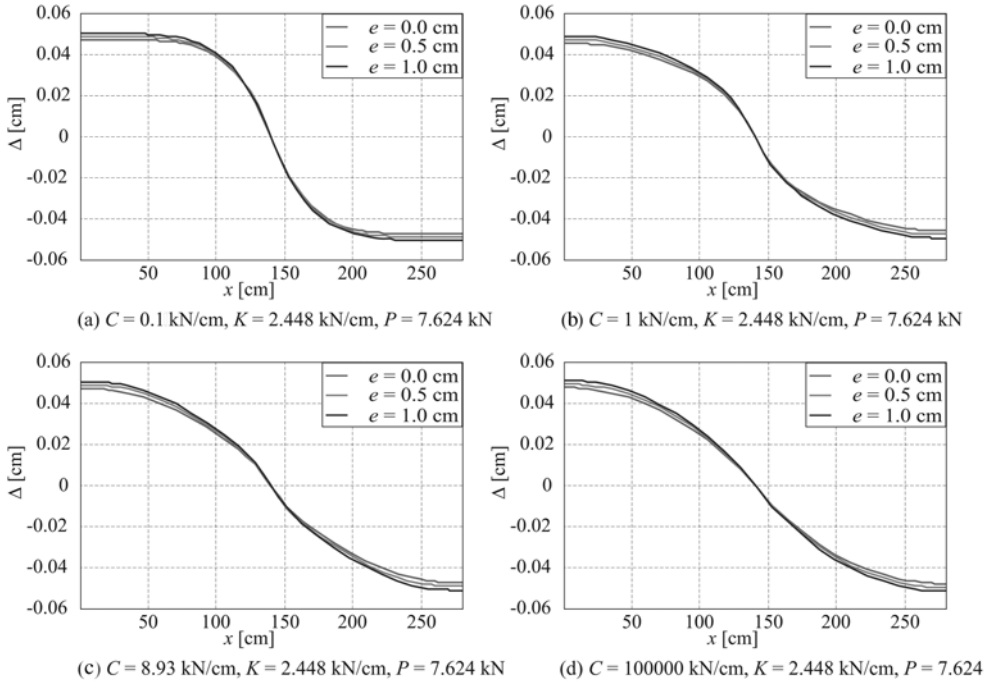

(a) $C = 0.1$ kN/cm, $K = 2.448$ kN/cm, $P = 7.624$ kN (b) $C = 1$ kN/cm, $K = 2.448$ kN/cm, $P = 7.624$ kN

(c) $C = 8.93$ kN/cm, $K = 2.448$ kN/cm, $P = 7.624$ kN (d) $C = 100000$ kN/cm, $K = 2.448$ kN/cm, $P = 7.624$

Fig. 8 Slip variation along the contact for various thicknesses of the connecting layer and for different transverse contact stiffnesses

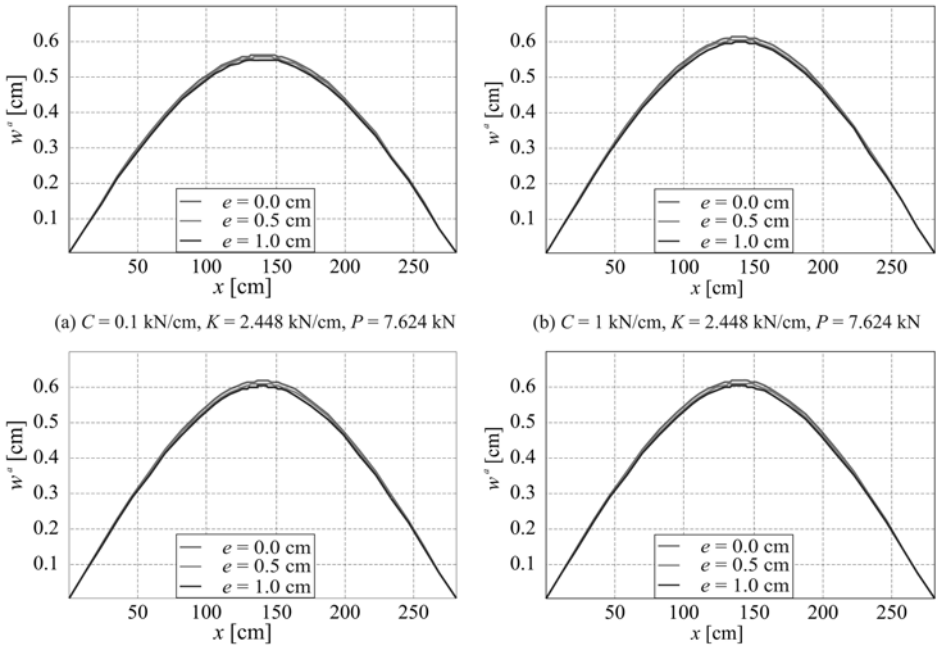

(a) C = 0.1 kN/cm, K = 2.448 kN/cm, P = 7.624 kN

(b) C = 1 kN/cm, K = 2.448 kN/cm, P = 7.624 kN

(c) C = 8.93 kN/cm, K = 2.448 kN/cm, P = 7.624 kN

(d) C = 100000 kN/cm, K = 2.448 kN/cm, P = 7.624 kN

Fig. 9 The variation of the deflection of the lower layer for various connecting layer thicknesses and for different transverse contact stiffnesses

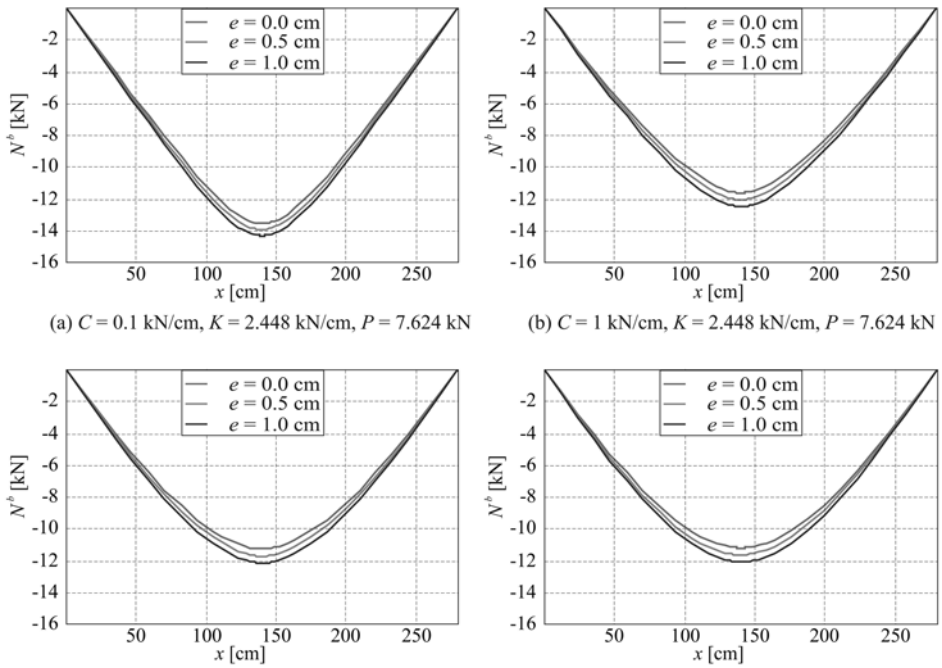

(a) C = 0.1 kN/cm, K = 2.448 kN/cm, P = 7.624 kN

(b) C = 1 kN/cm, K = 2.448 kN/cm, P = 7.624 kN

(c) C = 8.93 kN/cm, K = 2.448 kN/cm, P = 7.624

(d) C = 100000 kN/cm, K = 2.448 kN/cm, P = 7.624

Fig. 10 The variation of the axial force in the upper layer for various connecting layer thicknesses and for different transverse contact stiffnesses

transverse contact stiffness.

It is clear that the thickness of the connecting layer has practically no influence on slip.

The set of graphs in Fig. 9 presents the variation of the vertical deflection of the lower layer as a function of the thickness of the connecting layer for different transverse contact stiffnesses. Again, the effect is negligible.

Fig. 10 presents the variation of the axial force in the upper layer. It is clear that the effect of the thickness of the connecting layer on the axial force is negligible as well.

We may conclude that the effect of the thickness of the connecting layer on the strain and stress state of the nailed, two-layer timber beam can safely be neglected.

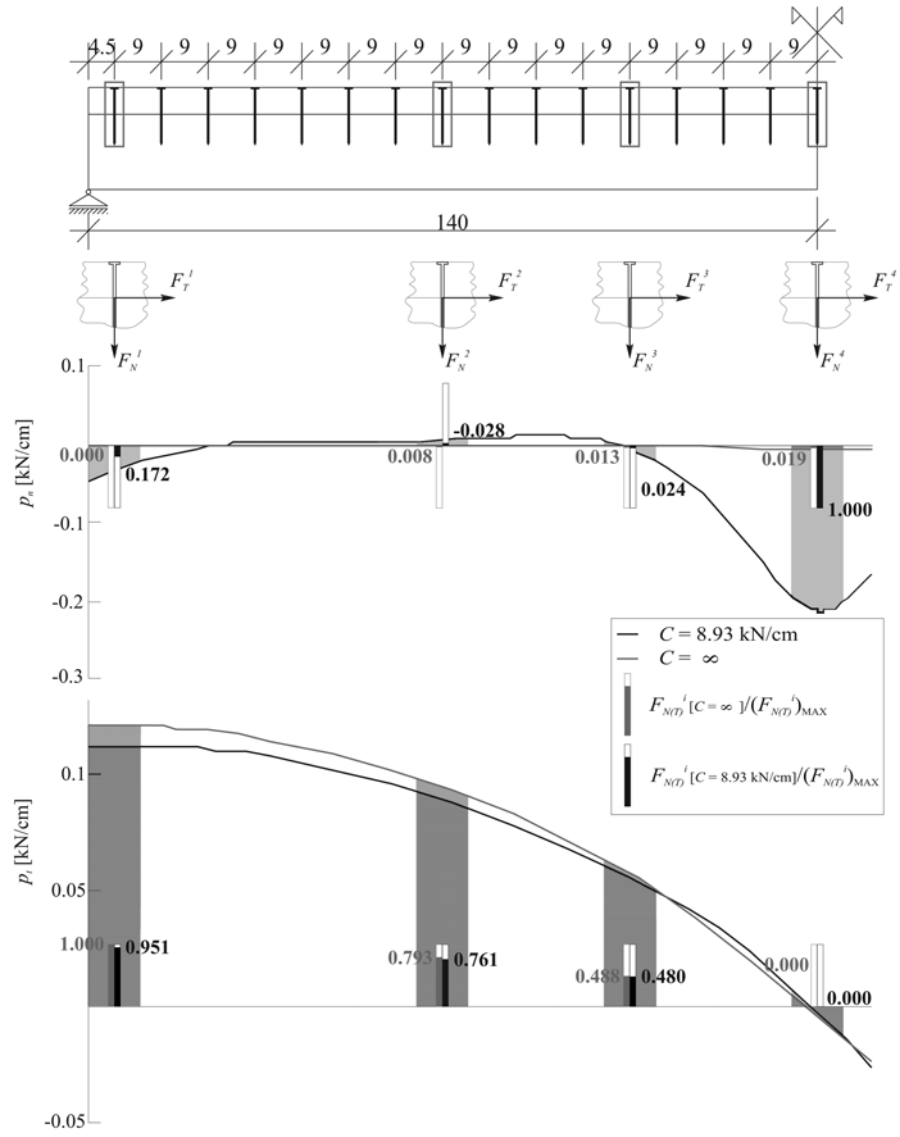

Fig. 11 The variation of nail forces for different transverse contact stiffnesses

3.3 The effect of transverse contact stiffness on nail forces

Fig. 11 shows the graphs of variation of the tractions, $p_n(x)$ and $p_t(x)$, at the beam contact surface, for the actual and the stiff transverse connection. There the hatched part of the graphs indicates how the force in the nail was computed from the surface forces. Fig. 11 also presents the values of forces in selected nails. They are given relative to the ultimate bearing capacity of the nail, separately for the transverse and for the shear direction, and presented in bar-like graphs. As expected the shear force in the nails is essentially independent on the transverse contact stiffness. In contrast, the effect of the transverse contact stiffness on the axial force in the nails is enormous at the point of the load application and is a lot larger in the case of the flexible connection.

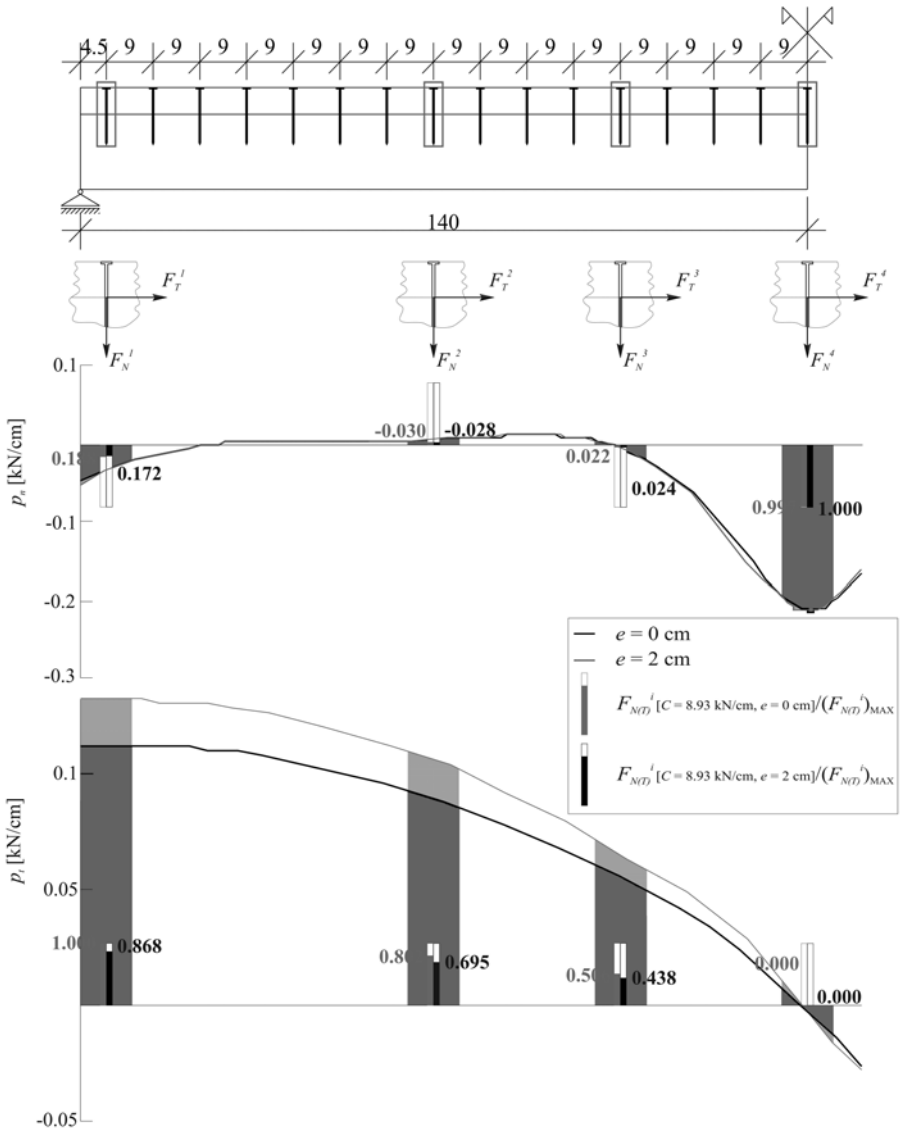

Fig. 12 Variation of nail forces for different connecting layer thicknesses

3.4 The effect of the thickness of connecting layer on nail forces

The analysis of forces in the selected nails has also been made for different values of the connecting layer thicknesses. Fig. 12 displays the results for two thicknesses: 0 and 2 cm. The axial forces in the nails are not sensitive to the thickness. Shear forces in the nails do differ somewhat, however; roughly a 15% drop of the shear force is observed at the ends of the beam for the 2 cm thick connecting layer.

4. Conclusions

An analytical solution of the deformation of a nailed, two-layer timber beam considering both slip and uplift has been presented. It is assumed that the timber layers are connected with each other by a thin elastic layer of a fictitious material with a small, but finite thickness. Such a generalization may sometimes improve the response of the model significantly. A similar thickness-like parameter has been introduced in a different way by Čas *et al*. (2004b).

The analytic solution makes us possible to carry out an extensive analysis of the effects of the transverse and the shear contact stiffnesses, and of the thickness of the connecting layer on the stress and strain state of two-layer beams. It has been established that:

- The transverse contact stiffness between the layers has some influence on the tangential contact surface traction, and largely dictates uplift at the contact interface at the point of the load application. It is somewhat surprising, however, that the transverse stiffness has only a minor influence on the rest of the equilibrium, deformation and kinematic quantities of structural engineer's interest. Consequently, the delamination can be neglected in engineering design if small displacements are assumed.
- The thickness of the connecting layer is also found to be a negligible parameter that does not contribute to the accuracy of the strain-stress state of two-layer timber beams. Thus, it can be neglected in the engineering analysis.
- The axial force in the nails close to the point of the load application of an external force could be very large for highly transversely flexible connections.

Acknowledgements

The work of A. Kroflič was financially supported by the Slovenian Research Agency (ARRS) under contract 1000-07-310191. The support is gratefully acknowledged.

References

Adekola, A.O. (1968), "Partial interaction between elastically connected elements of a composite beam", *Int. J. Solids Struct.*, **4**(11), 1125-1135.

Ayoub, A. (2005), "A force-based model for composite steel-concrete beams with partial interaction", *J. Constr. Steel Res.*, **61**(3), 387-414.

Betti, R. and Gjelsvik, A. (1996), "Elastic composite beams", *Comput. Struct.*, **59**(3), 437-451.

Čas, B., Saje, M. and Planinc, I. (2004a), "Non-linear finite element analysis of composite planar beams with an interlayer slip", *Comput. Struct.*, **82**, 1901-1912.
Čas, B., Saje, M., Bratina, S. and Planinc, I. (2004b), "Non-linear analysis of composite steel-concrete beams with incomplete interaction", *Steel Compos. Struct.*, **4**(6), 489-507.
Deo, S.G. and Ragmavendra, V. (1994), *Ordinary Differential Equations and Stability Theory*, 8th Edition, Tata McGraw-Hill Publishing Company Limited, New Delhi.
Eurocode 5 (2004), "Design of composite steel and concrete structures - Part 1-1: General rules and rules for buildings", European Committee for Standardization.
Fabbrocino, G., Manfredi, G. and Cosenza, E. (1999), "Non-linear analysis of composite beams under positive bending", *Comput. Struct.*, **70**, 77-89.
Fabbrocino, G., Manfredi, G. and Cosenza, E. (2000), "Analysis of continuous composite beams including partial interaction and bond", *J. Struct. Eng-ASCE*, **126**(11), 1288-1294.
Gara, F., Ranzi, G. and Leoni, G. (2006), "Displacement-based formulations for composite beams with longitudinal slip and vertical uplift", *Int. J. Numer. Meth. Eng.*, **65**(8), 1197-1220.
Gattesco, N. (1999), "Analytical modeling of nonlinear behavior of composite beams with deformable connection", *J. Constr. Steel Res.*, **52**, 195-218.
Girhammar, U.A. and Gopu, V.K.A. (1993), "Composite beam-columns with interlayer slip-exact analysis", *J. Struct. Eng-ASCE*, **119**(4), 1265-1282.
Girhammar, U.A. and Pan, D.H. (2007), "Exact static analysis of partially composite beams and beam-columns", *Int. J. Mech. Sci.*, **49**(2), 239-255.
Granholm, H. (1949), "On composite beams and columns with special regard to nailed timber structures", Trans. No. 88, Chalmers University of Technology, Goeteborg, Sweden (In Swedish).
Hirst, M.J.S. and Yeo, M.Y. (1980), "The analysis of composite beams using standard finite element programs", *Comput. Struct.*, **31**(1-2), 155-168.
Koc, P. and Štok, B. (2004), "Computer-aided identification of the yield curve of a sheet metal after onset of necking", *Comput. Mater. Sci.*, **11**(3), 233-237.
Manfredi, G., Fabbrocino, G. and Cosenza, E. (1999), "Modeling of steel-concrete composite beams under negative bending", *J. Eng. Mech-ASCE*, **125**(6), 654-662.
Milner, H.R. and Tan, H.H. (2001), "Modelling deformation in nailed, thin-webbed timber box beams", *Comput. Struct.*, **79**, 2541-2546.
Newmark, N.M., Seiss, C.P. and Viest, I.M. (1951), "Tests and analysis of composite beams with incomplete interaction", *Proc. Soc. Exp. Stress Anal.*, **9**(1), 75-92.
Nguyen, D.M., Chan, T.K. and Cheong, H.K. (2001), "Brittle failure and bond development length of CFRP-concrete beams", *J. Compos. Constr.*, **5**(1), 12-17.
Nie, J. and Cai, C.S. (2003), "Steel-concrete composite beams considering shear slip effects", *J. Struct. Eng-ASCE*, **129**, 495-506.
Oehlers, D.J., Nguyen, N.T., Ahmed, M. and Bradford, M.A. (1997), "Transverse and longitudinal interaction in composite bolted side-plated reinforced-concrete beams", *Struct. Eng. Mech.*, **5**(5), 553-563.
Pendhari, S.S., Kant, T. and Desai, Y.M. (2006), "Nonlinear analysis of reinforced concrete beams strengthened with polymer composites", *Struct. Eng. Mech.*, **1**(1), 1-18.
Planinc, I., Schnabl, S., Saje, M., Lopatič, J. and Čas, B. (2008), "Numerical and experimental analysis of timber composite beams with interlayer slip", *Eng. Struct.*, **30** (11), 2959-2969.
Pleshkov, P.F. (1952), "Theoretical studies of composite wood structures", Soviet Union (In Russian).
Rahimi, H. and Hutchinson, A. (2001), "Concrete beams strengthened with externally bonded FRP plates", *J. Compos. Constr.*, **5**(1), 44-56.
Ranzi, G., Bradford, M.A. and Uy, B. (2003), "A general method of analysis of composite beams with partial interaction", *Steel Compos. Struct.*, **3**(3), 169-184.
Ranzi, G. and Bradford, M.A. (2007), "Direct stiffness analysis of a composite beam-column element with partial interaction", *Comput. Struct.*, **85**(15-16), 1206-1214.
Rasheed, H.A. and Pervaiz, S. (2002), "Bond slip analysis of fiber-reinforced polymer-strengthened beams", *J. Eng. Mech-ASCE*, **128** (1), 78-86.
Rassam, H.Y. and Goodman, J.R. (1970), "Buckling behavior of layered wood columns", *Wood Sci.*, **2**(4), 238-

246.
Robinson, H. and Naraine, K.S. (1988), "Slip and uplift effects in composite beams", *Proceedings of an Engineering Foundation Conference ASCE*, New England College, Henniker, New Hampshire.
Salari, R., Spacone, E., Shing, P.B. and Frangopol, D.M. (1998), "Nonlinear analysis of composite beams with deformable shear connectors", *J. Struct. Eng-ASCE*, **124**(10), 1148-1158.
Salari, M.R. and Spacone, E. (2001), "Analysis of steel-concrete composite frames with bond-slip", *J. Struct. Eng-ASCE*, **127** (11), 1243-1250.
Schnabl, S., Planinc, I., Saje, M., Čas, B. and Turk, G. (2006), "An analytical model of layered continuous beams with partial interaction", *Struct. Eng. Mech.*, **22**(3), 263-278.
Schnabl, S., Saje, M., Turk, G.. and Planinc, I. (2007a), "Locking-free two-layer Timoshenko beam element with interlayer slip", *Finite Elem. Anal. Des.*, **43**(9), 705-714.
Schnabl, S., Saje, M., Turk, G.. and Planinc, I. (2007b), "Analytical solution of two-layer beam taking into account interlayer slip and shear deformation", *J. Struct. Eng-ASCE*, **133**(6), 886-894.
Seracino, R., Oehlers, D.J. and Yeo, M.F. (2001), "Partial-ineraction flexural stresses in composite steel and concrete bridge beams", *Eng. Struct.*, **23**, 1186-1193.
Stüssi, F. (1947), "Zusammengesetze Vollwandträger", *International Association for Bridge and Structural Engineering (IABSE)*, **8**, 249-269.
Sun, F.F. and Bursi, O.S. (2005), "Displacement-based and two-field mixed variational formulations for composite beams with shear lag", *J. Eng. Mech-ASCE*, **131**(2), 199-210.
Suzuki, H. and Chang, T.P. (1979), "Bending of laminated cantilever beams with interlayer slip", *J. Struct. Div.,* ASCE, **105** (2), 269-281.
Thompson, E.G., Googman, J.R. and Vanderbilt, M.D. (1975), "Finite element analysis of layered wood systems", *J. Struct. Div., Proc.* ASCE, **101**(12), 2659-2672.
Van Der Linden, M.L.R. (1999), "Timber-concrete composite beams", *HERON*, **44**(3), 215-239.
Viest, I.M. (1960), "Review of research on composite steel-concrete beams", *J. Struct. Div.* ASCE, **86**(6), 1-21.
Wang, Y.C. (1998), "Deflection of steel-concrete composite beams with partial shear interaction", *J. Struct. Eng-ASCE*, **124**(10), 1159-1165.
Wheat, D.L. and Calixto, J.M. (1994), "Nonlinear analysis of two-layered wood members with interlayer slip", *J. Struct. Eng-ASCE*, **120**(6), 1909-1929.
Wolfram Research Inc. (2005), *Mathematica*, Champaign, USA.
Xu, R.Q. and Wu, Y.F. (2007), "Two-dimensional analytical solutions of simply supported composite beams with interlayer slips", *Int. J. Solids Struct.*, **44**(1), 165-175.